Periodica Polytechnica
Civil Engineering

62(4), pp. 1039–1051, 2018
https://doi.org/10.3311/PPci.12512
Creative Commons Attribution

Nonlinear Normal Modes of a Piecewise Linear Continuous Structure with a Regular State

Róbert K. Németh[1*], Borbála B. Geleji[1]

RESEARCH ARTICLE

Received 09 May 2018; Revised 22 June 2018; Accepted 02 August 2018

Abstract

In this paper, the dynamic behaviour of a family of piecewise linear structures, namely the vibration of beams on block-and-tackle suspension system is analysed. The regularity of the vibration modes in one of the linear states induces non-harmonic, yet periodic free vibration modes. The periodicity constraint of the continuous structure is formulated using modal analysis in the regular state. The required number of modes in the finite modal analysis is specified so that the numerical damping caused by the omitted modes does not change the periodic or non-periodic nature of the free vibration of the continuous structure. It is shown, that the application of five excess passive modes allows to draw conclusions about the behaviour of the continuous structure. The periodic behaviour depends on the number and position of the suspension points and the number of the active vibration modes. Analysis of the limits of the periodic behaviour reveals that suspension points close to the middle of the beam, or first few active vibration modes result in periodic vibration of the nonlinear system.

Keywords

block-and-tackle suspension system, piecewise linear system, nonlinear normal mode

1 Department of Structural Mechanics,
Faculty of Civil Engineering,
Budapest University of Technology and Economics,
H-1521 Budapest, P.O.B. 91, Hungary
* Corresponding author, email: nemeth.robert@epito.bme.hu

1 Introduction

In case of structures with linear governing equations all vibration modes result in periodic (furthermore harmonic) motion, thus they can be depicted by closed curves in the phase space with period time depending on the mode only. A well-known property of these modal solutions is that the linear combination of them yields all solutions of the system [1, 2]. In nonlinear systems, this is typically not true. While there are possible periodic orbits, the period of these orbits is typically energy-dependent, and the amplitude-dependent modal shapes cannot serve as the basis of a linear modal analysis. The periodic vibration modes of the nonlinear system, called Nonlinear Normal Modes (NNM) have been known for a while, and raise several questions and interests, a recent overview of the topic can be found in [3]. The principle of superposition does not apply in energy- and thus amplitude-dependent NNMs, yet they can form a basis of the vibration analysis of nonlinear systems when harmonic or periodic excitation is considered [4, 5, 6]. One of the typical applications of the results is the reduction of the unwanted effects of large amplitude vibrations [7].

For piecewise linear Multi-Degree-Of-Freedom (MDOF) systems the modal analysis is still a possibility to introduce simplifications that facilitate the analysis of the system response [8, 9]. A crucial step in handling such systems is the change between the different linear phases. This can be done by the transformation of the modal displacements and velocities, for which a numerically effective method is shown in [10]. The physical background of the piecewise linear behaviour can be for instance the opening or closing of a crack or a gap, or a tightening and relaxation of a suspending cable.

For continuous, piecewise linear systems, a similar approach can be used. The linear regimes can be treated using modal analysis. In this case, the change between the linear states must be considered for an infinite number of modal coordinates [11]. Due to the orthogonality of the linear vibration modes, this transformation is linear and can be represented by a transformation matrix. For regular structures with pure analytical shape functions in each state this transformation matrix can be given analytically, but for a general problem the shape functions and

thus the transformation matrix can only be calculated numerically. Numerical computation of the transformation matrix also means the reduction of the modal space to finite dimension. Neglecting the higher modes introduces a numerical damping into the solution [12]. In [13], a general method was introduced to find periodic orbits based on modal analysis.

A piecewise linear continuous system, a linear elastic Euler-Bernoulli beam supported by two simple supports and a block-and-tackle suspension system is introduced in [12]. The massless cable is driven through a set of pulleys. Since the cable can only bear tension, the structure has two states called active and passive states depending on whether the cable exerts a force on the structure or it is slacked. Free vibration analysis of the structure was done in [14], initiating the beam from one of its active modal shapes. As the displacements and the velocities of the midpoint suggested, each of the four analysed active modal shapes result in a periodic vibration. The above periodicity is the consequence of the integer ratio of the eigenparameters to the first mode's eigenparameter in one of the linear states. Thus the periods of higher modes are integer quotients of the base period in that state, resulting in an integer number of half sine waves to occur during the half period of the first mode of that state. As the above property originates in the regular arrangement of the eigenparameters we will refer to such linear states as *regular states*. Starting the analysis from a passive modal shape did not give the same result, hence several questions arose about the generality of the existence of periodic vibration modes. As all examined active modes presented the periodic behaviour, it is supposed that this periodicity is the property of a larger set of initial modes.

This paper aims to answer the following questions regarding a family of structures derived from the one mentioned above. Is the existence of regular normal modes a general property of this family of structures, or the known solutions are a few of the rare exceptions? If it is a common property, what are the limits of existence of these regular nonlinear normal modes? Is it possible to characterize the behaviour of the continuous structure based on finite modal analysis? If so, what is the required number of considered passive modes to predict the behaviour of the continuous structure?

The paper is organized as follows. The mechanical system and its governing equations are presented in Section 2 along with the periodicity of the affected orbits. In Section 3, the numerical methods used to find the initial shapes resulting in a periodic vibration are presented. The numerical results are presented in Section 4, finally, the conclusions are drawn in Section 5.

2 Regular NNMs of a cable-suspended beam

2.1 Mechanical model of the cable-suspended beam

We investigate a family of simply supported beams, strengthened by a cable driven through an even number ($2c$) of pulleys attached to the beam (see an example with $c = 2$ in Fig.1).

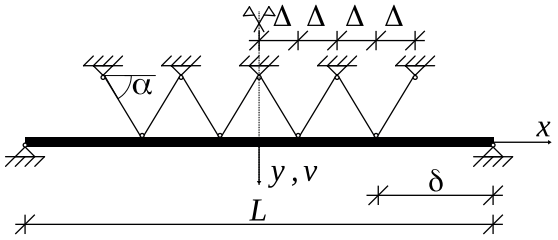

Fig. 1 One member of the analysed family of structures: $c = 2$.

The elongation and the mass of the cable are assumed to be negligible. The radius of the pulleys, their mass and friction are neglected as well, thus the cable force is constant along the whole cable. The assumption of small displacements is applied, hence the direction of the cable force is calculated on the initial geometry. Thus, the resultant of the cable force is the same vertical force at each suspension point. The constraint introduced to the system by the cable connects the displacements of multiple points of the structure, thus the reaction forces exerted by the cable form a one-parameter force system. Hence the order of static indeterminacy increases only by one. The effect of a similar support on the static behaviour of a cable net structure was analysed in [15].

The beam is an Euler-Bernoulli beam, the shear deformation of the cross sections is neglected. The partial differential equation of the free vibration for the $v(x, t)$ lateral translation of the beam axis is [16]:

$$\mu\ddot{v}(x,t) + EIv''''(x,t) = 0, \tag{1}$$

where μ is the specific mass, EI is the bending stiffness, $\dot{()}$ represents derivation with respect to time, and $()'$ represents derivation with respect to x.

The passive and active states of the cable are separated. In the *passive state*, the sum of the displacements of the suspension points cannot be positive, i.e.:

$$\sum_{i=1-c}^{c} v\big((2i-1)\cdot\Delta,t\big) \le 0, \tag{2}$$

and the displacement function is a single analytical function on the whole $-L/2 < x < L/2$ domain.

In the *active state*, the sum of the displacements of the suspension points equals zero, i.e.:

$$\sum_{i=1-c}^{c} v\big((2i-1)\cdot\Delta,t\big) = 0, \tag{3}$$

and the jump in the shear force is the same non-negative value at every i-th suspension point:

$$\lim_{\epsilon\to 0}\Big(EIv''''\big((2i-1)\cdot\Delta+\epsilon,t\big) - EIv''''\big((2i-1)\cdot\Delta-\epsilon,t\big)\Big) = 2S_y(t) \ge 0, \tag{4}$$

where $i = 1 - c, 2 - c, \ldots, c - 1, c$. Thus, the third derivative of the $v(x, t)$ function is not continuous, and $v(x, t)$ must be written for separate segments of various lengths.

It is assumed that the cable was attached to the system once the beam had reached equilibrium under the effect of self-weight. The displacements are measured with respect to this state. Note that in a more realistic scenario the cable would bear load already in the equilibrium state, and the static part of the load of a typical cable-stayed beam is large enough to avoid the slackening of the cable during the vibration.

2.2 Vibration modes of the linear subsystems

Separation of the variables $v(x, t) = u(x)h(t)$ in Eq.(1) yields the general form of the modal shape functions

$$u(x) = A\cos\left(\frac{\lambda x}{L}\right) + B\sin\left(\frac{\lambda x}{L}\right) + C\cosh\left(\frac{\lambda x}{L}\right) + D\sinh\left(\frac{\lambda x}{L}\right) \quad (5)$$

and the harmonic time-function

$$h(t) = b_c\cos(\omega_0 t) + b_s\sin(\omega_0 t). \quad (6)$$

Here λ is the non-dimensional eigenparameter and ω_0 is the natural circular frequency of the mode. Substitution of the derivatives of the assumed form of the solution in Eq.(1) yields that these two parameters are related through:

$$\omega_0^2 = \frac{\lambda^4 EI}{L^4\mu}. \quad (7)$$

The b_c and b_s modal parameters depend on the initial conditions. The *time period* of each mode is:

$$T_0 = \frac{2\pi}{\omega_0} = \frac{2\pi}{\lambda^2}\sqrt{\frac{L^4\mu}{EI}}. \quad (8)$$

Henceforth *a* and *p* superscripts are used to indicate the active and passive state of the cable, respectively.

For the *passive state* of the cable, the boundary conditions yield the *A*, *B*, *C* and *D* parameters: the translations in the support and the bending moments i.e. second derivatives in the supports are zero:

$$u\left(-\frac{L}{2}\right) = u\left(\frac{L}{2}\right) = u''\left(-\frac{L}{2}\right) = u''\left(-\frac{L}{2}\right) = 0. \quad (9)$$

In the *q*-th passive mode, the eigenparameter is

$$\lambda_q^p = q\pi \quad (10)$$

The eigenparameters are evenly spaced among the positive numbers, so we refer to the passive state as a *regular state*. The respective time periods are

$$T_{0q}^p = \frac{2}{q^2\pi}\sqrt{\frac{L^4\mu}{EI}}. \quad (11)$$

For odd values of *q*, $B_q^p = C_q^p = D_q^p = 0$, and A_q^p is arbitrary. To make the shape function unique, we normalize it to an $L^{(2)}$-norm. This results in the symmetric modal shape functions

$$u_q^p(x) = \sqrt{\frac{2}{L}}\cos\left(\lambda_q^p\frac{x}{L}\right). \quad (12)$$

For even values of *q*, $A_q^p = C_q^p = D_q^p = 0$, and B_q^p is arbitrary. To make the shape function unique, we normalize it to an $L^{(2)}$-norm. This results in the skew-symmetric modal shape functions

$$u_q^p(x) = \sqrt{\frac{2}{L}}\sin\left(\lambda_q^p\frac{x}{L}\right). \quad (13)$$

The structure remains in the passive state as long as the total elongation of the cable remains negative. The elongation of the cable in the *r*-th mode is caused by the translation of the suspension points, the sum of the projection of each translation on the connecting two cable segments results:

$$m_q = \sum_{i=1-c}^{c} u_q^p\left((2i-1)\Delta\right)\cdot 2\cdot\sin\alpha, \quad (14)$$

where α is the angle between the cable and the horizontal. For even values of *q* the skew-symmetric shape results $m_q = 0$. For the symmetric modes with odd values of *q*, considering Eqs.(12) and (10), the modal elongation will be:

$$m_q = \sqrt{\frac{32}{L}}\cdot\sin\alpha\cdot\sum_{i=1}^{c}\cos\left((2i-1)\Delta\frac{q\pi}{L}\right). \quad (15)$$

The total elongation of the cable during the passive state can be written as:

$$e(t) = \sum_{q=1}^{\infty} m_q\left(\eta_q^p\cos\left(\omega_{0q}^p t\right) + \frac{\zeta_q^p}{\omega_{0q}^p}\sin\left(\omega_{0q}^p t\right)\right). \quad (16)$$

In the *active state*, for each *j*-th segment between the suspension points there is a separate set of A_j, B_j, C_j and D_j parameters. The shape function given by these parameters satisfy the same boundary conditions as in the case of passive cable, and the segments fulfill the connection conditions in the suspension points. Each connection condition consists of two parts. The limits of the translation, the first and the second derivatives from left and right are the same (continuity condition), furthermore, the jumps in the third derivative are the same, since they are based on the jump in the shear force from the resultant of the cable forces. The λ_r^a eigenparameter is a result of this procedure, from which the respective periods are

$$T_{0r}^a = \frac{2\pi}{\left(\lambda_r^a\right)^2}\sqrt{\frac{L^4\mu}{EI}}. \quad (17)$$

To obtain unique solutions, the shape functions are scaled, with the purpose that the $L^{(2)}$-norm over the whole domain equals 1.

In both passive and active states, the vibration modes are either symmetric or skew-symmetric, for the proof in a specific case see the appendix of [12]. Skew-symmetric shapes are common for both states of the cable. For these modes, both the elongation of the cable and the cable force are zero. Such vibration modes are linear, they are not affected by the cable. In the further analysis, only the symmetric shapes are dealt with, thus the skew-symmetric parts are omitted. From now on, the *r* index always represents the *r*-th symmetric mode.

For the following steps of the analysis it is assumed that the λ_r^a eigenparameters and the $u_r^a(x)$ normalised modal shape functions for the active state, and the λ_r^p eigenparameters and the $u_r^p(x)$ normalised modal shape functions for the passive state are already computed. The ω_{0r}^a and ω_{0r}^p natural circular frequencies then can be calculated from Eq.(7). In Appendix A. we give the details of these calculations, where the elastic deformation of the cable is considered. The specific case of our analysis can be derived as a limit case, where the stiffness of the cable goes to infinity. The extensibility of the cable affects the calculation of the active modes only, the passive modes remain regular, so we expect that similar behaviour would occur in the case of structures with extensible cables, however the limits of the Δ parameter would be different.

As long as the cable remains in active state, the vibration of the beam can be written as

$$v(x,t)=\sum_{r=1}^{\infty}u_r^a(x)\left(\eta_r^a\cos\left(\omega_{0r}^a t\right)+\frac{\zeta_r^a}{\omega_r^a}\sin\left(\omega_{0r}^a t\right)\right), \qquad (18)$$

where η_r^a and ζ_r^a depend on the initial conditions at $t = 0$ (initial modal coordinates and initial modal velocities). Similarly, as long as the cable remains in the passive state, we can write:

$$v(x,t)=\sum_{r=1}^{\infty}u_r^p(x)\left(\eta_r^p\cos\left(\omega_{0r}^p t\right)+\frac{\zeta_r^p}{\omega_r^p}\sin\left(\omega_{0r}^p t\right)\right), \qquad (19)$$

where η_r^p and ζ_r^p are based on the initial conditions at $t = 0$ (initial modal coordinates and initial modal velocities).

We introduce the infinite vectors of modal initial conditions η_∞^a, ζ_∞^a and η_∞^p, ζ_∞^p for active and passive states, respectively. The $C_\infty^a(t)$ matrix is an infinite diagonal matrix, its r-th main diagonal element is $cos(\omega_{0r}^a t)$, the $S_\infty^a(t)$ matrix is an infinite diagonal matrix, its r-th main diagonal element is $sin(\omega_{0r}^a t)$. Similarly, matrices $C_\infty^p(t)$ and $S_\infty^p(t)$ have the same role in the passive state. The spectral matrices Ω_∞^a and Ω_∞^p are infinite diagonal matrices with the natural circular frequencies. Finally, the modal shape functions are assembled into the infinite $u_\infty^a(x)$ and $u_\infty^p(x)$ vectors. Using the above matrices and vectors, the displacement and the velocity function of the beam can be written as:

$$v^a(x,t)=u_\infty^{aT}(x)\left(C_\infty^a(t)\eta_\infty^a+S_\infty^a(t)\Omega_\infty^{a-1}\zeta_\infty^a\right), \qquad (20)$$

$$\dot{v}^a(x,t)=u_\infty^{aT}(x)\left(-S_\infty^a(t)\Omega_\infty^a\eta_\infty^a+C_\infty^a(t)\zeta_\infty^a\right) \qquad (21)$$

in the active state. The symbol ^{T} represents the transpose of a vector or a matrix. In the passive state, the matrix formulation becomes:

$$v^p(x,t)=u_\infty^{pT}(x)\left(C_\infty^p(t)\eta_\infty^p+S_\infty^p(t)\Omega_\infty^{p-1}\zeta_\infty^p\right), \qquad (22)$$

$$\dot{v}^p(x,t)=u_\infty^{pT}(x)\left(-S_\infty^p(t)\Omega_\infty^p\eta_\infty^p+C_\infty^p(t)\zeta_\infty^p\right) \qquad (23)$$

2.3 Switch between the active and passive states

When the state of the cable changes, the modal coordinates and the modal velocities need to be transformed. At time t_c of state change, the displacement and velocity functions can be written in both states, i.e., the right-hand sides of Eqs.(20) and (22) are equal, and so are the right-hand sides of Eqs.(21) and (23):

$$v^a(x,t_c)=v^p(x,t_c),\quad \dot{v}^a(x,t_c)=\dot{v}^p(x,t_c) \qquad (24)$$

For the transformation, we multiply both sides of these equations by $u_\infty^p(x)$ and integrate over the length of the beam. From the orthogonality and normalization of the passive modal shapes, the $\int_{-L/2}^{L/2}u_\infty^p(x)u_\infty^{pT}(x)dx$ term on the right-hand sides results in an infinite identity matrix. On the left-hand side, we introduce the T_∞ transformation matrix for a shortening of the $\int_{-L/2}^{L/2}u_\infty^p(x)u_\infty^{aT}(x)dx$ term. The elements of this transformation matrix are:

$$T_{ij}=\int_{-L/2}^{L/2}u_i^p(x)u_j^a(x)dx. \qquad (25)$$

The transformation matrix defined above then implies the following formulas for the transformation of the initial conditions:

$$T_\infty\left(C_\infty^a(t)\eta_\infty^a+S_\infty^a(t)\Omega_\infty^{a-1}\zeta_\infty^a\right)=C_\infty^p(t)\eta_\infty^p+S_\infty^p(t)\Omega_\infty^{p-1}\zeta_\infty^p \qquad (26)$$

$$T_\infty\left(-S_\infty^a(t)\Omega_\infty^a\eta_\infty^a+C_\infty^a(t)\zeta_\infty^a\right)=-S_\infty^p(t)\Omega_\infty^p\eta_\infty^p+C_\infty^p(t)\zeta_\infty^p \qquad (27)$$

In the current work, finite modal analysis is applied, thus the size of the diagonal matrices and vectors are reduced. This reduction is not necessarily the same for the active and the passive states. The vectors and matrices in the reduced system are denoted by dropping the infinity symbol. The number of considered active and passive modes define the size of the matrices. The omitted higher modes introduce a numerical damping in the calculation [12], so the number of used modes affects the accuracy of the calculation.

2.4 Properties of the regular periodic vibrations

Initiating the beam in the active state of the cable from the n-th symmetric modal shape, the beam reaches the $v(x,t)=0$ equilibrium position. At this instant, the cable enters the passive state, hence the velocities need to be transformed into the passive state's modal velocities.

In this passive state, each mode with a symmetric shape function has a time period which is the period of the first mode (the *fundamental period*) divided by an odd number's square (see Eqs.(10) and (7)). This regularity in the modal periods causes that as long as the state of the cable does not change during the half of the passive fundamental period, the movement of each passive modal coordinate is a mode-dependent odd number of sine half waves in time. Figure 2 shows a triplet of such functions and their combination.

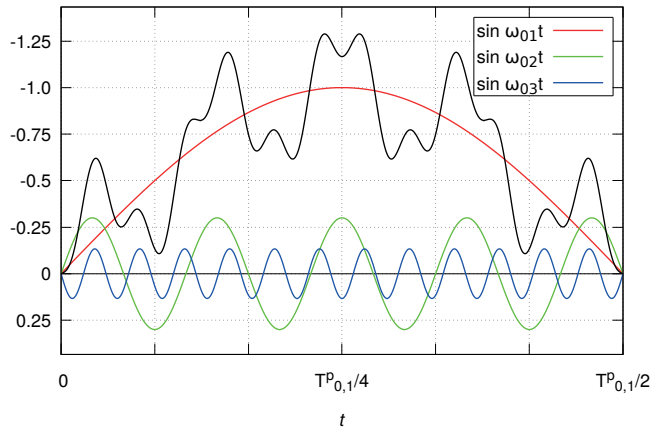

Fig. 2 Time-history of three modal co-ordinates and their sum throughout a passive half-period: the red, green and blue lines represent the displacement in the first, second and third passive mode, respectively, while the black line is their sum, and $T_{0,1}^{p}$ is the fundamental period.

Since the number of the half-waves is odd, the passive modal velocities at the end of this half-period are exactly the opposite of those at the beginning of the passive state. As the state of the cable changes back to active, the active modal velocities are the opposite of those before the previous state change. Thus, the amplitude of every other active mode will be zero, and the beam vibrates in the same active mode as it was initially released.

The cable remains slacked during the passive state of the half fundamental period. This slackening can be calculated using $e(t)$ defined in Eq.(16). To avoid the early change to an active state, it must be checked that the function does not become to positive during the passive half period. The question is if the vibration initiated from the n-th active mode transforms into the passive state such that the cable elongation in Eq. (16) does not become positive during the first passive mode. If the cable elongation remains non-positive, then the active modal shape of the continuous structure has the period

$$T_0 = T_{0n}^{a} + T_{01}^{p}. \tag{28}$$

The time periodicity of these modes is a consequence of the regularity of the passive modes, hence we refer to these modes as *Regular Nonlinear Normal Modes* (RNNM).

There is a set of exceptions from the above type of RNNMs. For certain structures, the shape functions of some symmetric passive modes of the beam coincide with the shape functions of symmetric active modes. In those passive modes, the m_r modal cable elongation is zero, and the same sinusoidal modal shape appears among the active and passive shapes with the same eigenparameters and natural frequencies. In these modes, both the modal cable elongation and the modal cable force is zero, and no distinction can be made between the two states. The vibrations in these modes remain linear, similarly to the case of skew-symmetric modal shapes, and the time period of these modes is T_{0n}^{a}. The formula of Eq.(28) would include multiple periods of the motion.

Numerically following the motion of the beam allows the consideration of a finite number of modes only. This causes a numerical damping in the calculation: the energy of the truncated passive modes is *numerically* dissipated. It is an open question if the infinite modal analysis would result in a periodic vibration. One possibility is that considering the neglected higher modes causes the cable elongation to become positive during the $T_{0,1}^{p}/2$ time, ruining the periodicity. The other option is that the higher modes do not change the passive state, and the consideration of infinite modes will decrease the energy loss to zero. Our goal is to propose a method on how the results of the reduced order model can be used to estimate the behaviour of the infinite modal analysis. Then the criteria on the existence of periodic modes are analysed.

3 Finding periodic modes of the generalized model

3.1 Characterization of the vibration in the passive state

The motion is started by initiating the beam from a symmetric active mode. In order to find modes that result in periodic motion, the elongation of the cable needs to be analysed. The sign of the elongation $e(t)$ of the cable during the passive fundamental half-period should not be positive. Considering the symmetry of the passive half-period in time, it is sufficient to analyse the time period of length $T_{0,1}^{p}/4$.

The initial active state is assumed to be the n-th mode with unit modal amplitude. To simplify the calculation, measuring the time is started at the first active-passive transformation. Then the S matrices become zero matrices and the C matrices become identity matrices, so transformations (26) and (27) simplify to:

$$\eta^{p} = T\eta^{a}, \quad \zeta^{p} = T\zeta^{a}. \tag{29}$$

From the assumption on the initial shape, the vector of modal translations is zero, while the vector of active modal velocities contains zero values except for the n-th component, which is $-\omega_{0,n}^{a}$, thus $\zeta^{a} = -\omega_{0,n}^{a} e_n$, where e_n is the n-th unit vector. The initial values of the passive modal velocities are $\zeta^{p} = -T\omega_{0,n}^{a} e_n = -T\Omega^{a} e_n$. With this notation, the elongation of the cable is

$$e(t) = -m^{T} S^{p}(t) \Omega^{p-1} T \Omega^{a} e_n, \tag{30}$$

where m is the vector containing the m_r modal elongations of the cable. Let us introduce the $T_2 = \Omega^{p-1} T \Omega^{a}$ matrix. Then T_{2rn} denotes the entry in the r-th row and n-th column of that matrix, and Eq.(30) can be simplified as

$$e(t) = -\sum_{r=1}^{k} m_r T_{2rn} \sin\left(\omega_{0,r}^{p} t\right), \tag{31}$$

where k is the number of passive modes considered (for the infinite analysis it would be infinity).

The definition of the T_2 matrix shows its effect: the coefficients of higher passive modes are always divided by the corresponding natural circular frequencies, so the effect of higher modes becomes negligible. One column of the T_2 matrix represents the amplitudes of the modal coordinates of the passive modes. These amplitudes multiplied by the modal cable elongations in the m vector define the coefficients of harmonic functions. The sum of these harmonic functions must be analysed for its maximum value in the analysed time range.

3.2 On the existence of periodic vibrations

Our goal is to quantify the negativity of $e(t)$. Since $e(0) = 0$, the maximum of $e(t)$ is not sufficient for this purpose, rather, its stationary values must be considered. For the approximate solution with k passive modes let e^k denote the maximum stationary value of $e(t)$, which occurs at $t_k \in \left(0; T^p_{0,1}/4\right]$ (i.e. $\dot{e}(t^k) = 0$). If the $e(t)$ function becomes positive during the analysed time, then e^k will be its maximum. If the $e(t)$ function remains non-positive during the analysed time, then the above definition of e^k skips the beginning of the motion. We justify the application of e^k by the fact that, in this latter case, the approximated $e(t)$ function starts decreasing after $t = 0$, and, as long as this function does not reach its first stationary point, it can not become positive.

For the numerical calculation of e^k, we propose the following method. The $\left(0; T^p_{0,1}/4\right]$ time domain is discretized in equal intervals at $t_i = i\Delta t$, and $e(t_i)$ are calculated. The interval Δt must be chosen such that the calculated values must follow sufficiently smoothly the highest considered passive mode.

In the numerical calculation of $e(t)$, only a finite number of modes can be considered. The proposed method allows a prognosis on the behaviour of a given mode. If there is no energy loss during the transformation, then a consecutive active-to-passive and passive-to-active transformation should provide the same active state as it was before the first transformation. Mathematically it means that the $T^T T$ product is an identity matrix. If there is an energy loss caused by the transformation, then the n,n entry of the $T^T T$ product:

$$t^k_{n,n} = \left[T^T T\right]_{n,n} \tag{32}$$

is smaller than one and represents the ratio of the kinetic energy remaining in the n-th active mode to the kinetic energy initially in the same mode. In a simple estimation on the error, we assume that all the disregarded energy is accumulating in the $(k + 1)$-th passive mode. In that case, every higher mode would have zero velocities, and from the assumption that no energy loss would occur in the infinite system implies that: $t^{k+1}_{n,n} = 1$. Thus, the maximal value of the $T_{k+1,n}$ entry is

$$T^{max}_{k+1,n} = \sqrt{1 - t^k_{n,n}}. \tag{33}$$

With this, the maximal amplitude from the $(k + 1)$-th passive mode can be calculated, according to Eq.(30) it is

$$d_k = m_{k+1} \frac{1}{\omega^p_{0,k+1}} T^{max}_{k+1,n} \omega^a_{0,n} \tag{34}$$

The maximum possible value of m_{k+1} is the number of the pulleys multiplied by the amplitude of the passive modal shape. This amplitude is the same for every k, from Eq.(12) it is $\sqrt{8/L} \cdot sin\alpha$, leading to

$$d_k = 2c \sin\alpha \cdot \sqrt{\frac{8}{L}} \frac{1}{\omega^p_{0,k+1}} T^{max}_{k+1,n} \omega^a_{0,n}. \tag{35}$$

Eq.(35) shows that the effect of higher modes is smaller, hence the assumption that all the truncated terms appear in the $(k+1)$-th mode gives an upper limit. The $sin\ \alpha$ term is a constant multiplier during the calculation of e^k and d_k. As we are primarily interested in the sign and ratio of these terms, its actual value is indifferent. Further calculations were done with $\alpha = 30°$.

Using estimation (35) on the amplitude of the truncated term in the $e(t)$ function, we can conclude that the n-th active shape results in an RNNM if the e^k critical value is negative and the d_k amplitude calculated with k passive modes is smaller than $-e^k$. In those cases, the critical point remains negative even with the added sinusoidal term. If the positive e^k critical value is larger than d_k then the critical value remains positive, and those modes cannot be considered as RNNMs. If the critical value is between $-d_k$ and d_k, then a further analysis of higher modes is required to decide whether the mode is an RNNM or not.

4 Results

4.1 The required number of passive modes to draw a conclusion on the periodicity

We analysed the stationary values e^k and the maximal differences d_k on a large number of active modes of various structures from the introduced family. The natural frequencies and modal shape functions of beams with 2, 4 and 6 suspension points (i.e. with $c = 1$, $c = 2$ and $c = 3$, respectively) with different positions of the pulleys were calculated. Then transformation matrices T and stationary values e^k were calculated with various number of passive modes (up to $k = 15$), initiating the beam from the n-th active mode with a unit modal amplitude at $t = 0$. To determine the stationary values e^k, the quarter-period of the passive state was divided into 6366 points, to compute values of $e(t)$. Thus, the full period of the fastest changing 15th mode was divided into 56 steps. So, the maximal difference between a sinusoidal function and its linear interpolation at the discrete points is $1 - cos\frac{2\pi}{2 \cdot 56} \approx 0.16\%$, and the error of the maximum of the function is in the same order of magnitude. The analysis was done for 535 active modes of structures with $c = 1$ and Δ varying between 0 and $L/2$, for 1129 active modes of structures with $c = 2$ and Δ varying between 0 and $L/6$, and for 477 active modes of structures with $c = 3$ and Δ varying between 0 and $L/10$. Every active mode was one of the first 6 modes.

First, the number of the required passive modes was analysed. The number of excess modes is defined as the difference between the considered number of passive modes and the index of the initial active mode, i.e. $k - n$. Figures 3–4 show the ratio of the maximal truncation error d_k to the maximal stationary value e^k as a function of the number of excess modes. Green points represent negative e^k: using these combinations, the vibration transforms with a smaller amplitude into the same single active mode as it was started, so these are the numerically damped periodic solutions. Red points represent positive e^k: these vibrations change back into the active mode earlier than the half-period of the first passive mode, hence they result in a nonperiodic free vibration. To follow the progress of the error while increasing the number of passive modes, the points are connected by lines. Green and red dashed lines connect the consecutive green and red points, respectively. Thin black lines connect consecutive points of different colours. These lines represent the number of applied passive modes, where the non-periodic vibration becomes periodic (or the periodic vibration becomes non-periodic) due to the inclusion of the next passive mode. This step typically changes the t^k instant of the stationary point, and the change often occurs near the $k \approx n$ value. The frequency of the n-th active mode is close to the frequency of the $(n + 1)$-th passive mode, the corresponding modal shapes are typically similar to each other, so the T matrix has relatively large values right below its main diagonal. Thus, by passive modes near the $(n + 1)$-th one have a significant effect on the instant of the stationary point of the infinite system, the inclusion of the k-th passive modes (i.e. where $k = n + 1$) play a crucial role in the calculation. This is the reason why the $k < n$ part of these graphs were not drawn.

The points of the sinusoidal vibration modes were also omitted. As it was mentioned earlier, in these modes the elongation of the cable is constant zero in the passive mode as well, thus the maximum of the d_k/e^k cannot be calculated.

The graphs allow deciding whether a number of passive modes are enough to draw conclusions about the behaviour of the continuous structure. Function values with higher absolute

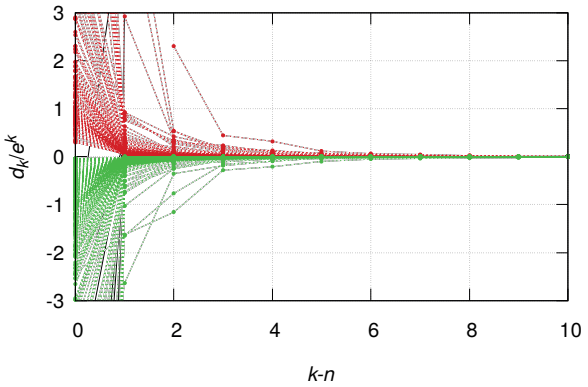

Fig. 3 Relative errors as a function of the excess modes for $c = 1$ structures. Each line represents one of the first 6 active modes of a structure with a specific Δ.

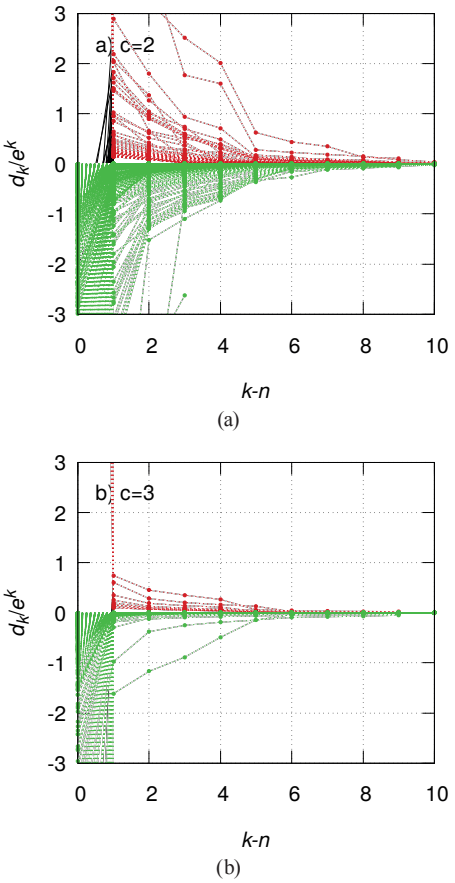

Fig. 4 Relative errors as a function of the excess modes for a) $c = 2$ and b) $c = 3$. Each line represents one of the first 6 active modes of a structure with a specific Δ.

value than one mean insufficient number of passive modes to decide periodicity, the inclusion of more passive modes is required. If the position of the stationary point does not change radically, then a function value between 0 and 1 represents the non-periodic modes. Under the same circumstances, a function value between –1 and 0 represents a periodic mode. The conclusion based on this property is that there is wide range of periodic and non-periodic solutions. Using at least $n + 5$ passive modes, the periodicity of the resulting motion does not change anymore.

4.2 Beams suspended on two points

The next step is the analysis of the $c = 1$ case, where the symmetric vibration of the beam can be treated in the same way as a three-span girder with partial middle supports which exert reactions only upwards.

Figure 5 shows the stationary values e^k as the function of the position Δ of the pulleys is varied between its physically possible values. Each calculation was done with 15 passive modes, the different colours represent the result of different starting modes. Boxed points represent the maximum stationary value for periodic modes $e^k < 0$, while stars represent the maximum stationary value calculated for active modes with non-periodic behaviour, $e^k > 0$. Empty circles denote the modes where the stationary value is zero ($e^k = 0$). A small change of Δ typically

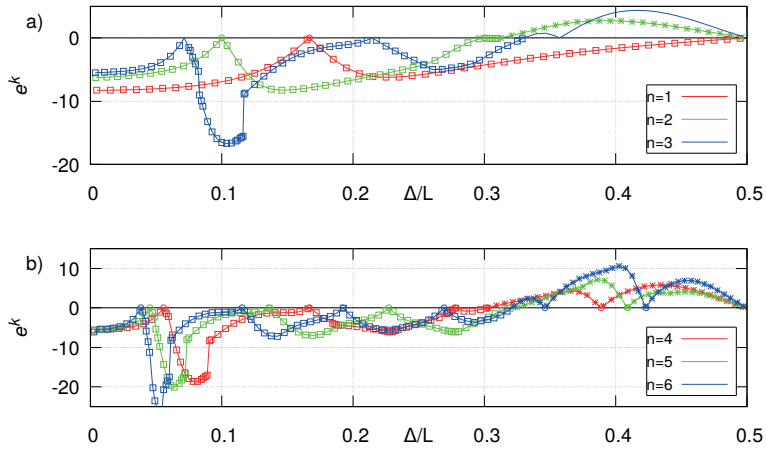

Fig. 5 The e^k stationary values of different active modes for $c = 1$ structures as a function of the position of pulleys for various initial modes n.

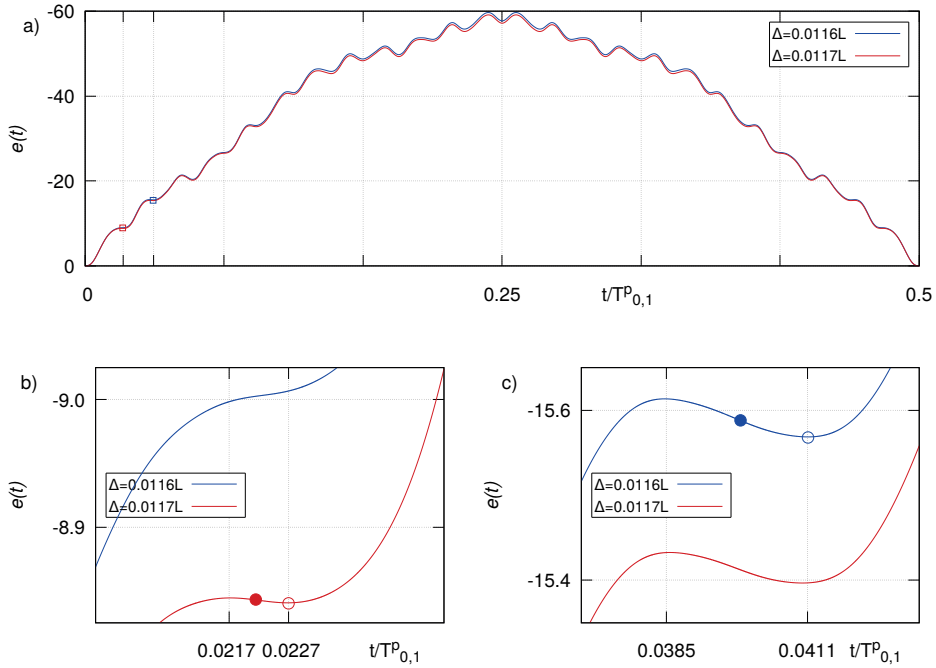

Fig. 6 a) Time-histories of two $e(t)$ functions of a $c = 1$ structure during the passive state of the $n = 3$ mode. Small boxes drawn around the stationary points are magnified below. b) The same functions around the stationary point of the $\Delta = 0.117L$ structure. c) The same functions around the stationary point of the $\Delta = 0.116L$ structure. The empty circles represent the stationary points, and the full circles the inflection points right before them.

only has a small effect on the vibration mode and the passive modal amplitudes, thus the calculated points were connected with linear segments.

The graph shows that stationary values of the first mode (red line in Figure 5.a)) are never positive. This means that, independent of the position of the suspension points, the first mode is always periodic. The typical behaviour for higher initial modes is that a large Δ results in positive e^k and thus non-periodic vibration, while smaller Δ results in negative e^k and thus periodic vibration. The transition occurs around $\Delta \approx 0.3L$, for some modes it happens in one single transition, while for some modes there are isolated regions with periodic or non-periodic behaviour.

A structure with $\Delta = L/6$ has the same mechanical behaviour as the structure analysed in [12] and [14]. The suspension points above the supports do not interact with the beam. The six points in Fig.5 at $\Delta = L/6$ represent two sinusoidal active modal shape (with $n = 1$ and $n = 4$), and four RNNM (with $n = 2$, $n = 3$, $n = 5$ and $n = 6$), in compliance to the results of [14].

The graphs in Fig.5 have curved segments, where the instant of the stationary point changes smoothly. These segments are separated by sudden jumps (e.g., the $n = 3$ case has one between $\Delta = 0.116L$ and $\Delta = 0.117L$). At these points, the stationary point with larger e^k ceases to exist as Δ is varied, and a stationary point with smaller e^k appears at a different t^k instant. To explain this jump, the time-history of the $e(t)$ functions of two vibrations is shown in Figure 6.a.: the $n = 3$ mode of the already mentioned $\Delta = 0.116L$ and $\Delta = 0.117L$ structures. Figure 6.b. shows $e(t)$ around the stationary point of the $\Delta = 0.117L$ highlighting that there is an inflection point before the first stationary point, denoted by a full and an empty circle, respectively. As the slope of the function at the inflection point

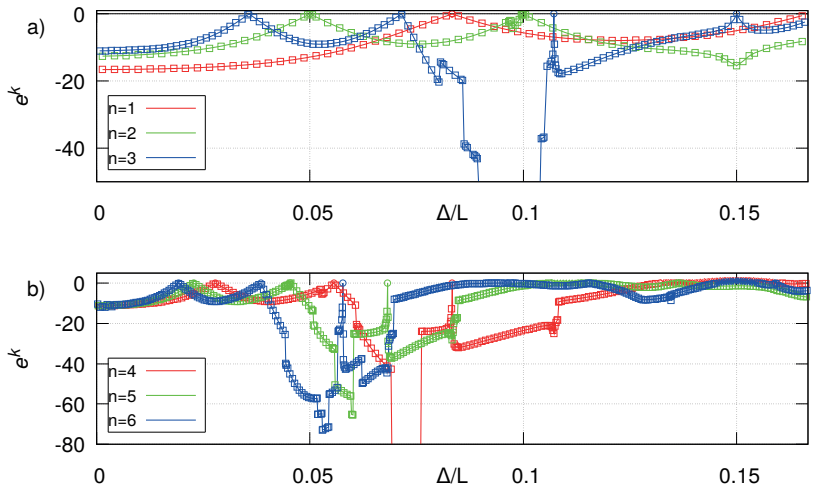

Fig. 7 The e^k stationary values of different active modes for $c = 2$ structures.

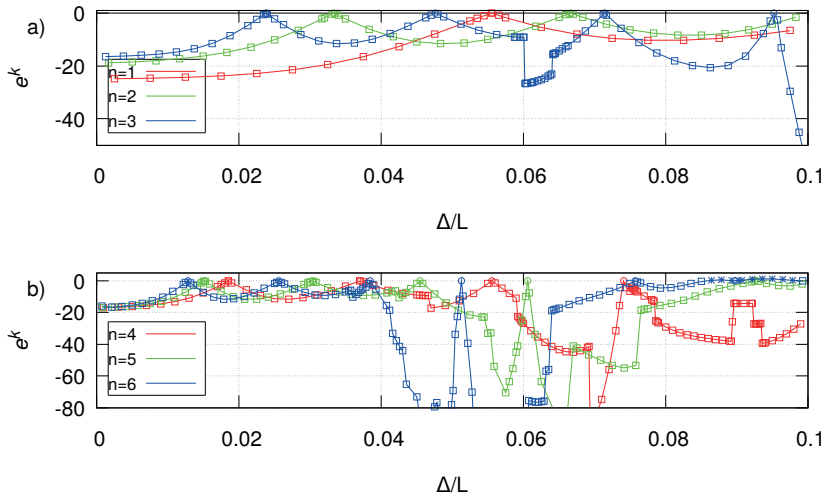

Fig. 8 The e^k stationary values of different active modes for $c = 3$ structures.

changes sign, the stationary point after the inflection vanishes. At $\Delta = 0.116L$, there is no stationary point anymore, the next candidate for this purpose is at a different time instant. This is shown on Figure 6.c. around the stationary point of a structure with $\Delta = 0.116L$.

Another type of the singularities can be observed in the graphs at the $e^k = 0$ points, where the slope of the function changes sign. A few examples are at $\Delta = L/6$ for $n = 1$, at $\Delta = L/10$ and $\Delta = 3L/10$ for $n = 2$, at $\Delta = L/14$, $\Delta = 3L/14$ and $\Delta = 5L/14$, for $n = 3$. These points belong to trivial normal modes, their distribution follows the regular pattern of $\Delta/L = (2j - 1)/(4n + 2)$ with integer j. As it was shown in [17], these active modes have pure sinusoidal vibration shapes, which coincide with one of the passive modes as well. Thus, no distinction can be made between the active and passive state and the period will be T^a_{0n}, which differs from the limit value, calculated from the left or from the right along the function with Eq.(28).

4.3 Beams suspended at more than two points

Figures 7 and 8 show the stationary values e^k as a function of the position Δ of the pulleys varied between its physically possible values for the $c = 2$ and $c = 3$ structures, respectively. Each calculation was done with 15 passive modes, the different colours represent the results of different starting active modes. Boxed points represent the maximum stationary value for periodic modes $e^k < 0$, while stars represent the maximum stationary value calculated for active modes with non-periodic behaviour, $e^k > 0$. Empty circles denote the modes where the stationary value is zero $e^k = 0$.

For $c = 2$, the first three active modes have no positive values, for $c = 3$ the first five modes have no positive value. It means that these active modes result in RNNMs independent of the position of the pulleys. This is a generalization of our former finding for the $c = 1$ case. The conjecture that the first $2c - 1$ mode is always an RNNM would require an extensive numerical testing, which is out of the scope of this paper.

The conclusion that was drawn on the higher modes of the c = 1 structures can be generalized as well. As long as Δ is sufficiently small, the higher active modes result in regular vibration modes. The positive e^k stationary points do not appear below the $\Delta = 0.1L$ point for $c = 2$ and below the $\Delta = 0.08L$ point for $c = 3$. While these limits depend strongly on the number of pulleys, it is worth noting that positive e^k and thus nonperiodic vibration occurs only when the last pulley is at a distance of

$0.3L - 0.5L$ from the center of the beam. So we formulate the conjecture that as long as $(2c - 1)\Delta < 0.3L$, initiating the structure from any active mode results in periodic vibration.

The limit case of $\Delta \to L/6$ represents, again, the same structure analysed in [12] and [14]. The graphs of $n = 1$ and $n = 4$ modes approach zero as $\Delta \to L/6$, while the graphs of higher modes have a negative value on the $\Delta = L/6$ end.

There are jumps in the calculated functions $e^k(\Delta/L)$, which have the same background as that explained in relation to Fig. 6. The zero limit values at the trivial normal modes have the same mechanical explanation as in the $c = 1$ case.

One new phenomenon worth noting is the kinks at some points (e.g. at $\Delta/L = 0.15$ in the $n = 3$ curve of Figure 7.a.). These points are not related to a sudden jump, a continuous function reaches these values. Furthermore, we observed, that the modes with these local minimums can be paired with a trivial normal mode, which has zero e^k value. The frequencies of these two modes are relatively close to each other, for the above mentioned $c = 2$ structure with $\Delta/L = 0.15$ the eigenparameters are $\lambda_2^a = 4.868\pi$ and $\lambda_3^a = 5\pi$. The non-smooth function of the stationary values might be caused by the non-separated modes of the active state.

5 Conclusions

In this paper, we gave an explanation of a phenomenon occurring during the free vibration of a piecewise linear structure with regular natural frequencies in one state. We have shown that there is a wide range of system parameters where nonlinear periodic vibrations occur, but there are active modes resulting in non-periodic vibration as well. The piecewise linear system we investigated is a beam suspended at 2, 4 or 6 points by a cable driven through a set of equidistant pulleys. The symmetric topology of the pulleys resulted in symmetric and skew-symmetric vibration modes only. As every skew-symmetric modal shape results in a trivial harmonic vibration mode, only the symmetric modal shapes were analysed.

We have introduced a stationary value to measure the periodicity of the vibration without the need for an infinite modal analysis. The partial modal analysis of the continuous system neglects higher order modes. We derived the maximal amplitude of the first truncated mode. The ratio of this maximal amplitude to the stationary value allowed us to draw conclusions on the periodic or non-periodic motion of the continuous system. Based on numerical studies, we gave a recommendation on the number of necessary passive modes in a numerical calculation with reduced modes.

A systematic study of the stationary values allowed us to draw conclusions on the periodicity of the vibration modes. We concluded that, depending on the number of suspension points, the first few active modes result in a regular nonlinear normal mode. The higher modes might result in non-periodic motion, but for sufficiently small distances between the pulleys, the motion remains periodic.

The periodic vibration modes support further analysis of NNMs. As the suspension allows the construction of slender structures, the analysis of forced vibration plays an important role in the design process. The periodic free vibration modes presented in this research lay the foundation of that analysis. Experimental validation of the current results requires the beam to be released from an active modal shape, which requires the application of static displacements according to that modal shape. This is an impractical task, but future analysis of the forced vibration offers the possibility to validate our prospective results.

The analysis presented in this paper neglects the mass of the cable. The actual mass of the cable would affect the results in several ways. In both states, the cable would perform a free vibration as a string. In the passive state, the motion of the cable is independent of the beam. In the active state, the motion of the cable and the motion of the beam is connected. Furthermore, the equilibrium state of the cable would be a catenary, which introduces a nonlinearity in the response of the structure in the active state. Consideration of all the above effects would modify the analytical calculation of the active and passive modal shapes, and possibly the regular distribution of the passive modes, thus it is beyond the scope of this paper.

Acknowledgement

The present study was supported by the National Research, Development and Innovation Office (grant K 119440).

References

[1] Den Hartog, J. P. "*Mechanical Vibrations*". Civil, Mechanical and Other Engineering Series. Dover Publications, 1985.

[2] Thomson, W. "*Theory of Vibration with Applications*". Taylor & Francis, 1996.

[3] Renson, L., Kerschen, G., Cochelin, B. "Numerical computation of nonlinear normal modes in mechanical engineering". *Journal of Sound and Vibration*, 364, pp. 177–206. 2016. https://doi.org/10.1016/j.jsv.2015.09.033

[4] Rosenberg, R. M., Kuo, J. K. "Nonsimilar normal mode vibrations of nonlinear systems having two degrees of freedom". *ASME*, *Journal of Applied Mechanics*, 31(2), pp. 283–290. 1964. https://doi.org/10.1115/1.3629599

[5] Rand, R. H. "A direct method for non-linear normal modes". *International Journal of Non-Linear Mechanics*, 9(5), pp. 363–368. 1974. https://doi.org/10.1016/0020-7462(74)90021-3

[6] Vakakis, A. F. "Non-linear normal modes (nnms) and their applications in vibration theory: An overview". *Mechanical Systems and Signal Processing*, 11(1), pp. 3–22. 1997. https://doi.org/10.1006/mssp.1996.9999

[7] Vakakis, A. F., Gendelman, O. V., Bergman, L. A., McFarland, D. M., Kerschen, G., Lee, Y. S. "*Non-linear Targeted Energy Transfer in Mechanical and Structural Systems*". Solid Mechanics and Its Applications. Springer Netherlands, 2008. https://doi.org/10.1007/978-1-4020-9130-8

[8] Shaw, S. W., Holmes, P. J. "A periodically forced piecewise linear oscillator". *Journal of Sound and Vibration*, 90(1), pp. 129–155. 1983. https://doi.org/10.1016/0022-460X(83)90407-8

[9] Jiang, D., Pierre, C., Shaw, S. W. "Large-amplitude non-linear normal modes of piecewise linear systems". *Journal of Sound and Vibration*, 272(3–5), pp. 869–891. 2004. https://doi.org/10.1016/S0022-460X(03)00497-8

[10] Yu, S. D. "An efficient computational method for vibration analysis of unsymmetric piecewise-linear dynamical systems with multiple degrees of freedom". *Nonlinear Dynamics*, 71(3), pp. 493–504. 2013. https://doi.org/10.1007/s11071-012-0676-8

[11] Lengyel, G., Németh, R. K. "Free vibration of a cracked, pre-stressed continuous rod". *Procedia Engineering*, 161, pp. 1656–1661. 2016. https://doi.org/10.1016/j.proeng.2016.08.641

[12] Kocsis, A., Németh, R. K., Turmunkh, B. "Dynamic analysis of a beam on block-and-tackle suspension system: A continuum approach". *Engineering Structures*, 101, pp. 412–426. 2015. https://doi.org/10.1016/j.engstruct.2015.07.022

[13] Lengyel, G., Németh, R. K. "Symmetric free vibration of a cracked, quasi-continuous, masonry arch". *Meccanica*, 53(4–5), pp. 1071–1091. 2018. https://doi.org/10.1007/s11012-017-0776-0

[14] Németh, R. K., Kocsis, A. "Csigasorral függesztett gerenda szabadrezgése modálanalízissel (Modal analysis of the free vibration of a beam on a block-and-tackle suspension system)". In: *XII. Magyar Mechanikai Konferencia*, pp. 1–12. (Szirbik, S., Baksa, A., Bertóti, E. (Eds.)) (in Hungarian), Miskolci Egyetem Gépészmérnöki és Informatikai Kar Műszaki Mechanikai Intézet, 2015

[15] Hincz, K. "Nonlinear analysis of cable net structures suspended from arches with block and tackle suspension system, taking into account the friction of the pulleys". *International Journal of Space Structures*, 24(3), pp. 143–152. 2009. https://doi.org/10.1260/026635109789867643

[16] Weaver, W., Timoshenko, S. P., Young, D. H. "*Vibration Problems in Engineering*". A Wiley-Interscience publication. John Wiley & Sons, 1990.

[17] Németh, R. K., Geleji, B. "Függesztett gerendacsalád szabadrezgése II.: Frekvenciatérkép számítása és vizsgálata, (Free vibration of a family of suspended beams II. Calculation and analysis of the frequency map)". *Építés- Építészettudomány*, 46(3–4), pp. 351–370. (in Hungarian) 2018. https://doi.org/10.1556/096.2017.006

[18] Geleji, B., Németh, R. K. "Függesztett gerendacsalád szabadrezgése I.: Sajátfrekvenciák és rezgésalakok számítása, (Free vibration of a family of suspended beams I. Calculation of natural frequencies and modal shapes)". *Építés- Építészettudomány*, 46(1–2), pp. 201–219. (in Hungarian) 2018. https://doi.org/10.1556/096.2017.005

Appendix A. Frequency matrix of a beam with active suspension system

In this Appendix, we present the systematic approach we derived and used for the calculation of the frequency matrix, the eigenparameters and the modal shape functions of the beam on a block-and-tackle suspension system with the active state of the cable. However, in the paper we were dealing with an inextensible cable, as a general approach, the following derivation considers the elastic deformation of the cable, so this is an extension to the algorithm shown in [18]. To determine the $u_r^a(x)$ functions for the active state of the beam suspended on $2c$ points (see Fig.1), we have to divide the function into sections at the coordinates of the pulleys. Each of these modal shapes must fulfill Eq. (1) and can be written in the form of Eq. (5). The parameters must be given for each segment, so we introduce the subscript l to distinguish between the segments. In the l-th segment, the function has the form

$$u_{r,l}^a(x) = A_l \cos\left(\frac{\lambda x}{L}\right) + B_l \sin\left(\frac{\lambda x}{L}\right) + C_l \cosh\left(\frac{\lambda x}{L}\right) + D_l \sinh\left(\frac{\lambda x}{L}\right), \tag{36}$$

and the function is valid between the x_{l-1} and x_l coordinates. The x_l coordinates represent both ends of the beam and the suspension points with $x_0 = -L/2$, $x_{2c+1} = L/2$ and $x_l = (2l - 2c - 1)\Delta$ for $l = 1,\ldots,2c$. The A_l, B_l, C_l and D_l parameters can be calculated from the boundary and the continuity conditions of the beam.

These conditions can be formulated in a much simpler form if we introduce a ζ_l local reference system with a simple translation: $\zeta_l = x - x_{l-1}$. The shape function of the given segment will be:

$$u_{r,l}^a(x) = U_{r,l}^a(\xi). \tag{37}$$

From here on we omit the a superscript and r subscript. The segment can be written as:

$$U_l(\xi) = J_l \cos\left(\frac{\lambda \xi}{L}\right) + K_l \sin\left(\frac{\lambda \xi}{L}\right) + L_l \cosh\left(\frac{\lambda \xi}{L}\right) + M_l \sinh\left(\frac{\lambda \xi}{L}\right), \tag{38}$$

with the following relationship between the coefficients:

$$\begin{aligned} A_l &= J_l \cos(x_{l-1}) - K_l \sin(x_{l-1}) \\ B_l &= J_l \sin(x_{l-1}) + K_l \cos(x_{l-1}) \\ C_l &= L_l \cosh(x_{l-1}) - M_l \sinh(x_{l-1}) \\ D_l &= -L_l \cosh(x_{l-1}) + M_l \sinh(x_{l-1}) \end{aligned} \tag{39}$$

The advantage of the translated coordinate system is that the constraints are written for function values only at $\xi = 0$, $\xi = 2\Delta$ and $\xi = \delta$ points (see Fig.1 for the meaning of Δ and δ).

Now the boundary and continuity conditions are given in detail. First, the simply supported beam has pinned support at both ends. This means that the deflection and the bending moment is zero at these points. This latter one is proportional to the second derivative of the deflection, hence the conditions can be written in the following form:

$$U_1(0) = 0, \quad U_1''(0) = 0, \tag{40}$$

$$U_{2c+1}(\delta) = 0, \quad U_{2c+1}''(\delta) = 0. \tag{41}$$

The next group of equations represent the continuity of the beam at the suspension points. The translation, the rotation and the bending moment must be the same on the left and right-hand side of each suspension points. As the rotation is related to the first derivative of the translation, while the bending moment is proportional to the curvature, and thus to the second derivative of the translation, these conditions can be written as:

$$U_1(\delta) = U_2(0), \quad U_1'(\delta) = U_2'(0), \quad U_1''(\delta) = U_2''(0), \tag{42}$$

for the first suspension point and as:

$$U_l(2\Delta) = U_{l+1}(0), \quad U_l'(2\Delta) = U_{l+1}'(0), \quad U_l''(2\Delta) = U_{l+1}''(0) \tag{43}$$

for every other suspension point with $l = 2,\ldots,2c$. For brevity, we simplified the equations by the constant terms EI and λ/L.

The last group of equations represents the jump in the shear force. The shear force is proportional to the third derivative of the translation, and the jump must be the same in each suspension point. We compare each jump to the first one:

$$U_1'''(\delta) - U_2'''(0) = U_l'''(2\Delta) - U_{l+1}'''(0) \tag{44}$$

for every suspension point with $l = 2, 3, \ldots, 2c$.

The last condition states that the vertical force transmitted from the cable to the beam is equal to the jump in the shear force. The latter one is proportional to the jump in the third derivative in any of the suspension points:

$$V_{jump} = EI\left(U_1'''(\delta) - U_2'''(0)\right), \tag{45}$$

where EI is the bending stiffness of the beam. The vertical force is calculated from the elongation of the cable, which can be calculated from the translations of the suspension points with:

$$\Delta\ell = \sum_{l=1}^{2c} U_{l+1}(0) \cdot 2 \cdot \sin\alpha. \tag{46}$$

The sinα term projects the translation to the direction of the cable, while 2 is the number of sloped cable segments in each suspension point. Let s denote the stiffness of the cable, so the cable force will be $S = s \cdot \Delta\ell$, its vertical component $S_y = S \cdot \sin\alpha$. There are two cable segments connecting to the suspension point so we can write short $2S_y = V_{jump}$. Substituting the partial results, we can write the last condition as:

$$\frac{EI}{4s\sin^2\alpha}\left(U_1'''(\delta) - U_2'''(0)\right) = \sum_{l=1}^{2c} U_{l+1}(0). \tag{47}$$

The assumption of the cable's inextensibility means, that s is infinite, and the right-hand side of Eq. (47) becomes zero. From the formula one can see that the validity of the assumption of an inextensible cable depends on the EI/s ratio.

Equations (40–47) can be written in a homogeneous form using (38) yielding the linear algebraic equation system:

$$Fc = 0. \tag{48}$$

Here vector $c = [J_1, K_1, L_1, M_1, J_2, K_2, L_2, M_2, \ldots M_{2c+1}]^T$ consists of the unknown coefficients and F is the frequency matrix containing the above-described continuity and boundary conditions. These conditions can be written in blocks that help understanding the structure of the frequency matrix. This way the frequency matrix in case of $c = 2$ has the form:

$$F=\begin{bmatrix}
\tilde{P} & 0_{2\times4} & 0_{2\times4} & 0_{2\times4} & 0_{2\times4}\\
0_{2\times4} & 0_{2\times4} & 0_{2\times4} & 0_{2\times4} & P\\
-\beta\tilde{C} & -\beta D+L & L & L & L\\
\tilde{A} & B & 0_{3\times4} & 0_{3\times4} & 0_{3\times4}\\
0_{3\times4} & A & B & 0_{3\times4} & 0_{3\times4}\\
\tilde{C} & D+C & -D & 0_{1\times4} & 0_{1\times4}\\
0_{3\times4} & 0_{3\times4} & A & B & 0_{3\times4}\\
\tilde{C} & D & C & -D & 0_{1\times4}\\
0_{3\times4} & 0_{3\times4} & 0_{3\times4} & A & B\\
\tilde{C} & D & 0_{1\times4} & C & -D
\end{bmatrix}, \tag{49}$$

where $\beta = EI\lambda^3/4s\sin^2\alpha L^3$ and the matrix blocks are the following: $0_{m\times n}$ denotes the $m \times n$ zero matrix,

$$\tilde{P}=\begin{bmatrix}1 & 0 & 1 & 0\\ -1 & 0 & 1 & 0\end{bmatrix},$$

$$P=\begin{bmatrix}\cos(\lambda\delta) & \sin(\lambda\delta) & \cosh(\lambda\delta) & \sinh(\lambda\delta)\\ -\cos(\lambda\delta) & -\sin(\lambda\delta) & \cosh(\lambda\delta) & \sinh(\lambda\delta)\end{bmatrix},$$

$$\tilde{C}=\begin{bmatrix}\sin(\lambda\delta) & -\cos(\lambda\delta) & \sinh(\lambda\delta) & \cosh(\lambda\delta)\end{bmatrix},$$

$$D=\begin{bmatrix}0 & 1 & 0 & -1\end{bmatrix}.$$

$$L=\begin{bmatrix}1 & 0 & 1 & 0\end{bmatrix},$$

$$\tilde{A}=\begin{bmatrix}\cos(\lambda\delta) & \sin(\lambda\delta) & \cosh(\lambda\delta) & \sinh(\lambda\delta)\\ -\sin(\lambda\delta) & \cos(\lambda\delta) & \sinh(\lambda\delta) & \cosh(\lambda\delta)\\ -\cos(\lambda\delta) & -\sin(\lambda\delta) & \cosh(\lambda\delta) & \sinh(\lambda\delta)\end{bmatrix}, \tag{50}$$

$$A=\begin{bmatrix}\cos(2\lambda\Delta) & \sin(2\lambda\Delta) & \cosh(2\lambda\Delta) & \sinh(2\lambda\Delta)\\ -\sin(2\lambda\Delta) & \cos(2\lambda\Delta) & \sinh(2\lambda\Delta) & \cosh(2\lambda\Delta)\\ -\cos(2\lambda\Delta) & -\sin(2\lambda\Delta) & \cosh(2\lambda\Delta) & \sinh(2\lambda\Delta)\end{bmatrix},$$

$$B=\begin{bmatrix}-1 & 0 & -1 & 0\\ 0 & -1 & 0 & -1\\ 1 & 0 & -1 & 0\end{bmatrix},$$

$$C=\begin{bmatrix}-\sin(2\lambda\Delta) & \cos(2\lambda\Delta) & -\sinh(2\lambda\Delta) & -\cosh(2\lambda\Delta)\end{bmatrix},$$

In Eq.(49), the block-row starting with $\tilde{P}$ represents Eq.(40), the block-row starting with $0_{2\times4}$ represents Eq. (41), the row starting with $\beta\tilde{C}$ represents Eq.(47), the block-row starting with $\tilde{A}$ represents Eq.(42), the block-rows starting with $0_{3\times4}$ represent Eq.(43) and the rows starting with $\tilde{C}$ represent Eq.(44).

The homogeneous Eq.(48) has nontrivial solutions if and only if the determinant of the frequency matrix is zero: $|F| = 0$. The matrix always can be partitioned into four blocks:

$$F=\begin{bmatrix}R & S\\ W & U\end{bmatrix} \tag{51}$$

with an 8×8 upper left block R and the respective S, W and U matrices. It can be shown that the lower triangular hypermatrix U is not singular, so the determinant can be calculated as: $|F| = |U| \cdot |R - SU^{-1}W|$. The nonlinear equation $|F| = 0$ must be solved for the λ eigenparameters, then the J_1, K_1, L_1, M_1 parameters can be computed from the homogeneous equation, which can be transformed to the A_1, B_1, C_1, D_1 values with Eq.(39).